InSAR results from the WInSAR Consortium

Matt Pritchard (1); Eric Fielding (2); Shimon Wdowinski (3); Scott Baker (4); Zhong Lu (5); and 160 WInSAR Institution members (6)
1: Cornell University;
2: Jet Propulsion Lab, Caltech;
3: University of Miami;
4: UNAVCO
5: Southern Methodist University
6: Various institutions worldwide

Prepared by: **Zhong Lu**, Chair, WInSAR Executive Committee

Outline of talk:

- What is WInSAR ?
- Research highlights from WInSAR members

What is WInSAR ?

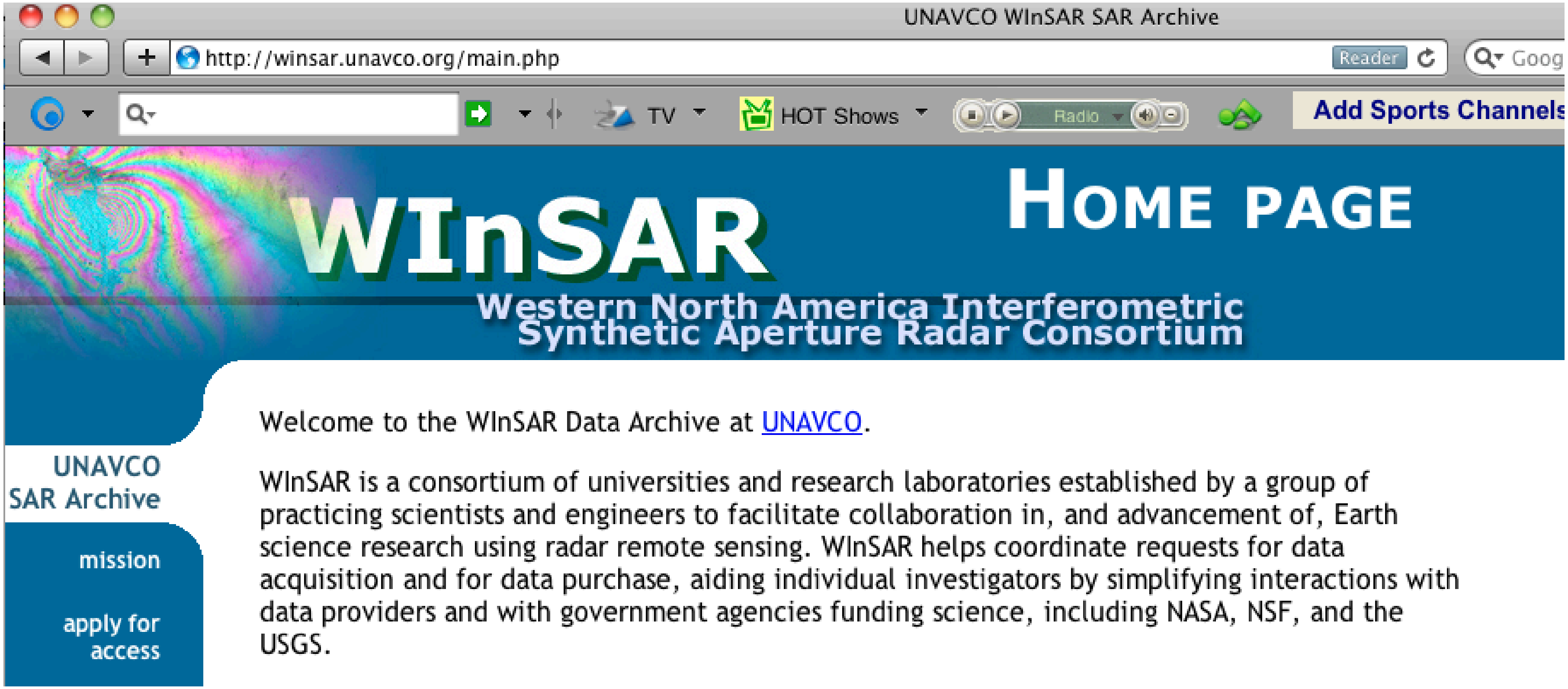

- **Consortium of more than 160 Universities & Research Institutions**
- **Executive Committee (elected, 2-year terms)**
- **Hosted by UNAVCO in Boulder, Colorado. UNAVCO provides organizational and operational support for WInSAR activities, including membership administration, financial management, data management and archiving, and software tools for data exploration and access.**

Funding:

WInSAR objectives

- Promote the use and development of InSAR technology for scientific investigations.
- Promote free and open access to SAR data as allowed by data providers.
- Acquire, archive and catalog SAR data of the U.S. active areas.
- Solicit funds and promote programs and space missions to meet these objectives.
- Mandate for sharing data among co-investigators comes from research funding agencies (NSF and NASA)

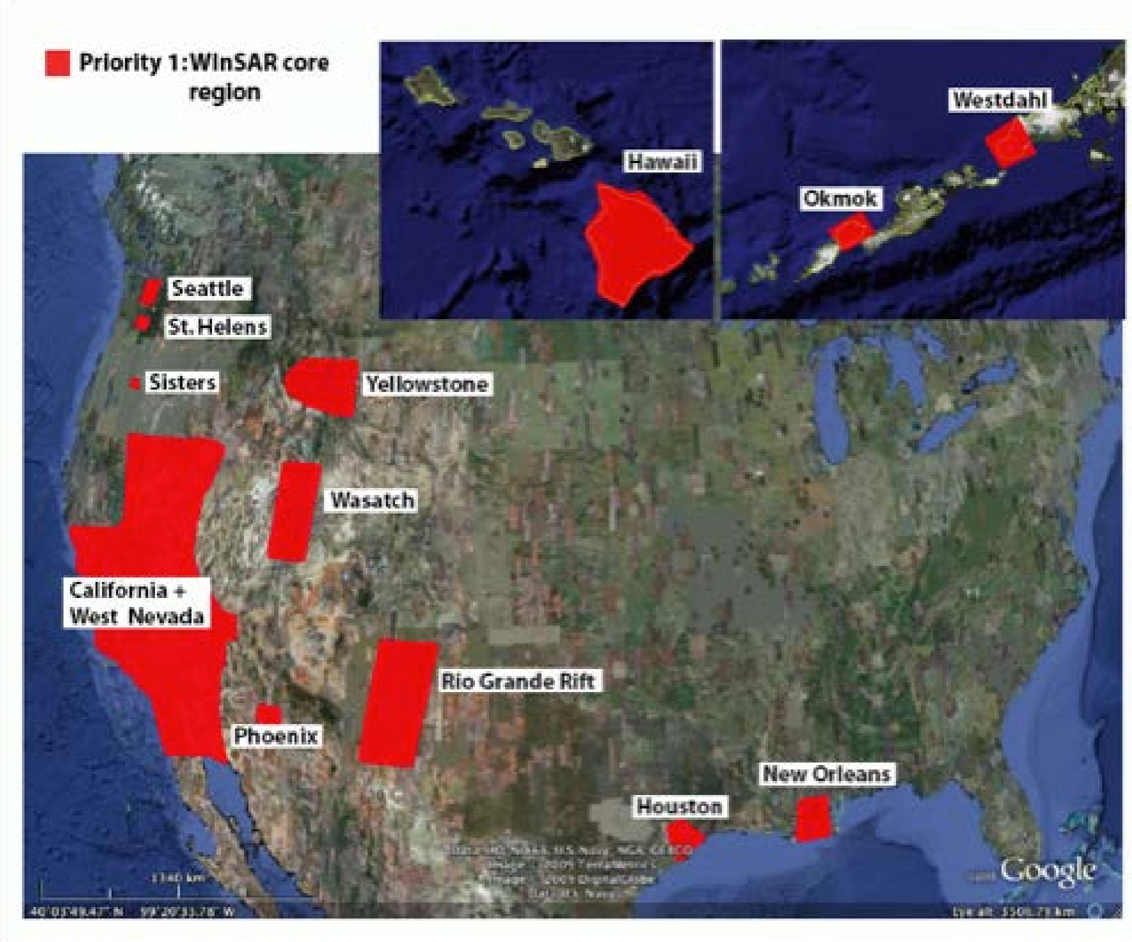

Why join WInSAR?

(#1 and #2 apply to US scientists only, for now)

#1) Access to SAR (ERS-1, ERS-2, Envisat, Radarsat-1, ALOS-1 data at UNAVCO (>20 Tb) after signed agreements.

#2) Facilitate co-principal investigators to share data (e.g.TSX) via UNAVCAO facility.

#3) Access to free open-source software: Once a license agreement is signed, WInSAR members can download the ISCE software for InSAR data processing that includes the mdx visualization software: http://winsar.unavco.org/isce.html

#4) Membership in a self-governing community:
News from WInSAR mailing list
Annual SAR/InSAR trainings
Annual WInSAR meeting/lunch at AGU
Input into use of resources for data purchase and access

Highlights of InSAR results from WInSAR members in past ~ 2 years.

1. Volcanoes

Pressurized magma reservoir within the east rift zone of Kīlauea Volcano, Hawai ʻi: Evidence for relaxed stress changes from the 1975 Kalapana earthquake

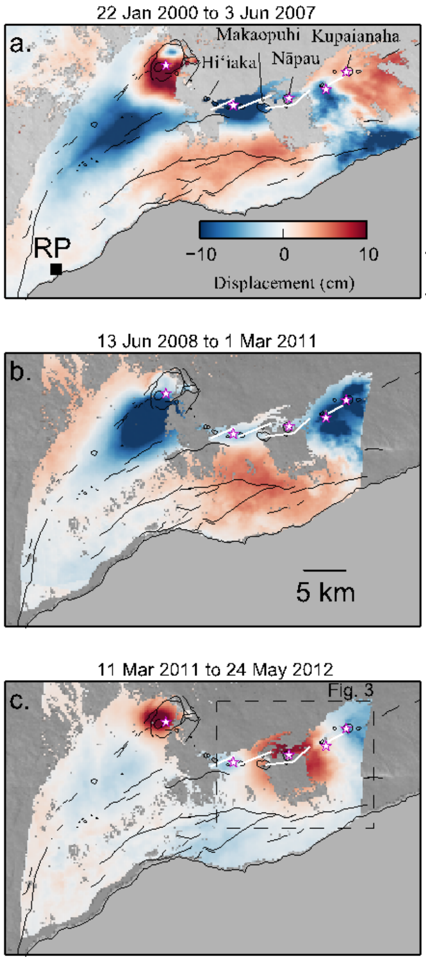

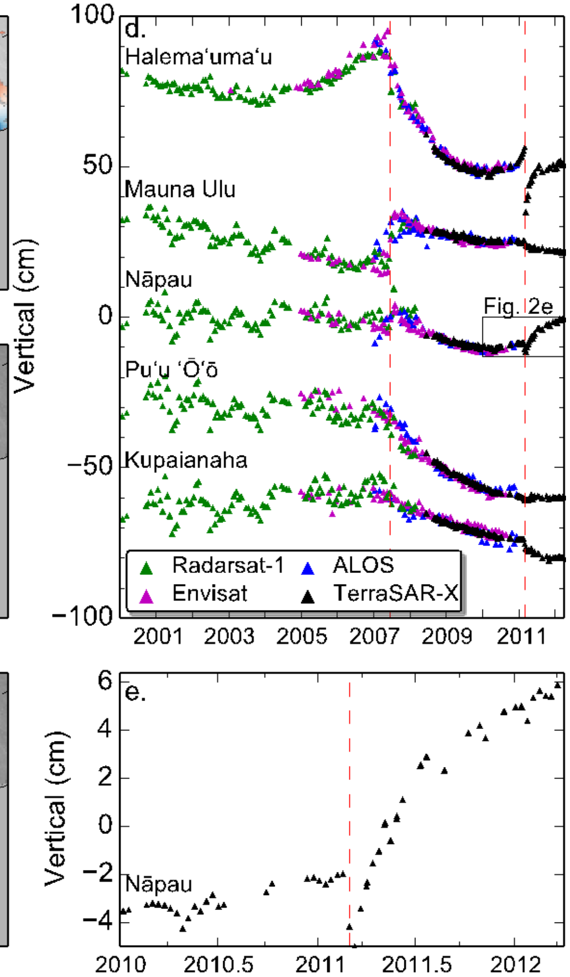

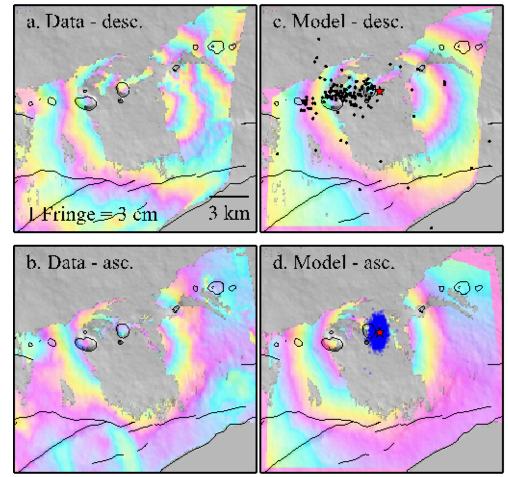

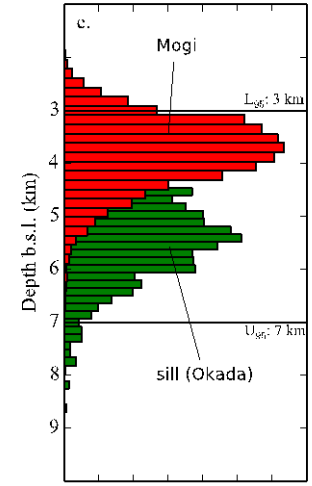

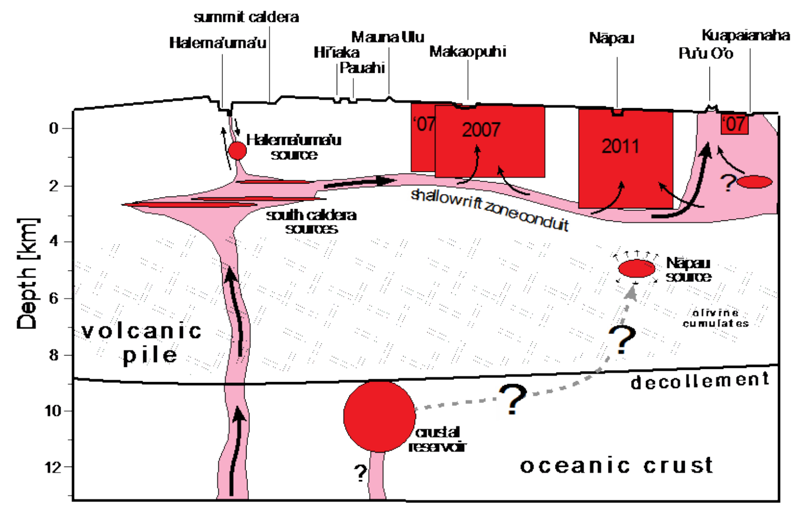

Baker, S., and F. Amelung (2015), Pressurized magma reservoir within the east rift zone of Kīlauea Volcano, Hawai ʻi: Evidence for relaxed stress changes from the 1975 Kalapana earthquake, Geophys. Res. Lett., 42, doi:10.1002/2015GL063161.

Three-dimensional secular surface-displacement maps by integrating multi-stacked Instar and MAI displacements from ascending and descending orbits

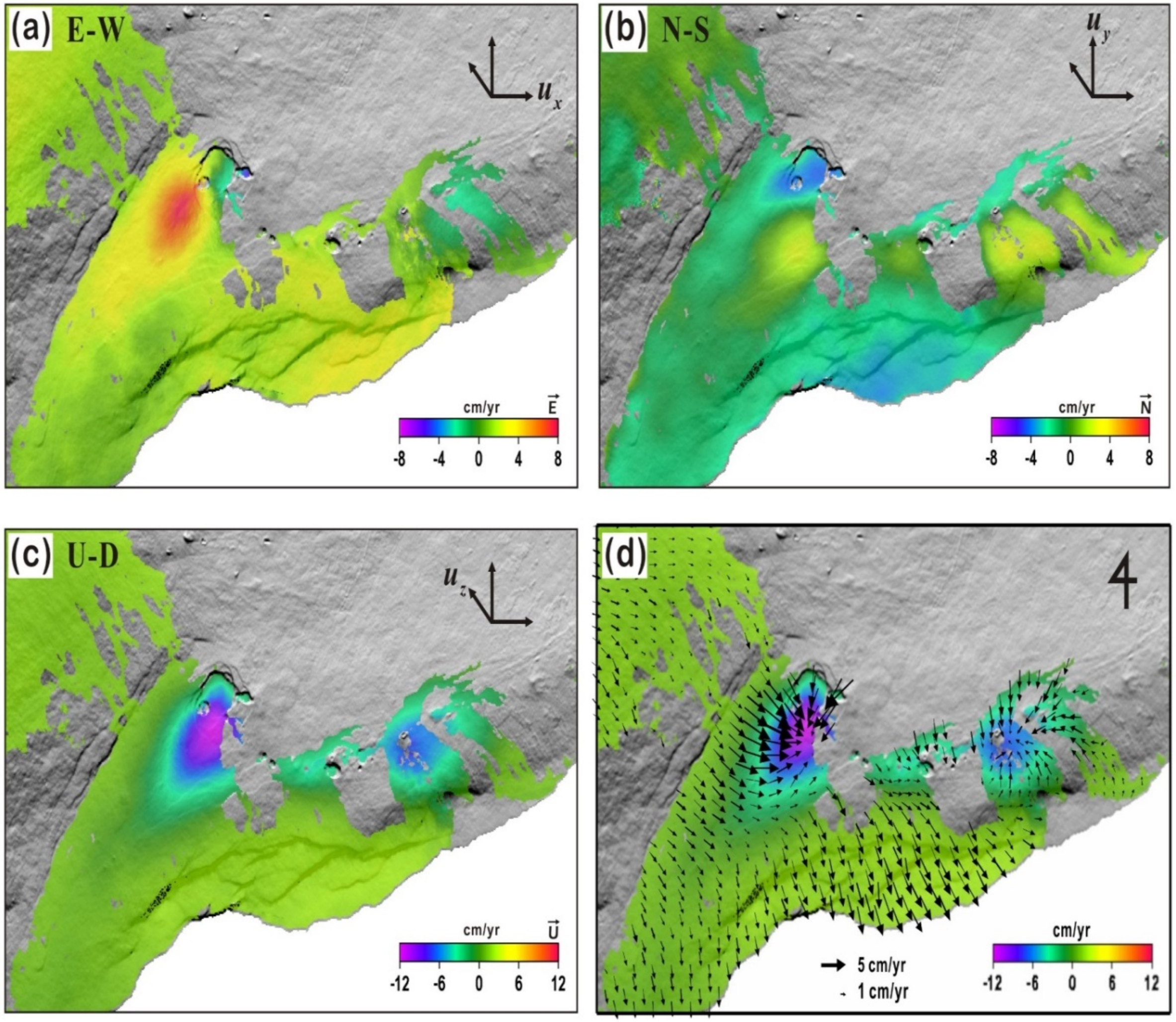

- **11 Envisat images from 1 descending track**
- **10 Envisat images from 1 ascending track**
- **Accuracy reaches to ~1 cm/year**

Jo et al., J. Geod, 2015

InSAR Imaging of Aleutian Volcanoes

- ✓ **ERS-1, ERS-2, JERS-1, Radarsat-1, Envisat, ALOS, TerraSAR-X imagery of 1990s-2010**
- ✓ **25,000 InSAR images plus modeling & analysis**

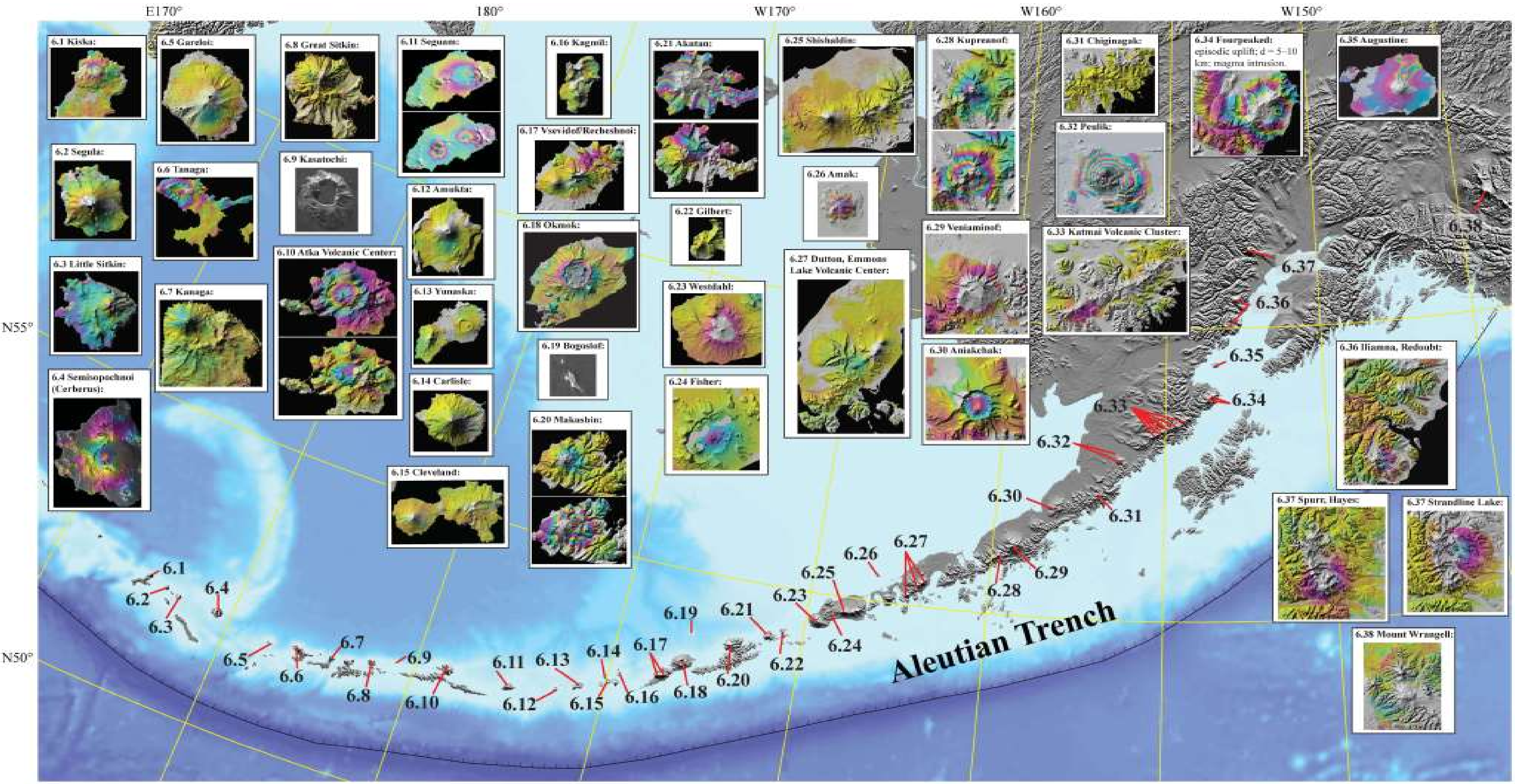

- **Lu and Dzurisin, Springer, 390 pp., 2014**

2. Interseismic

Southern San Andreas: localized vs distributed surface creep

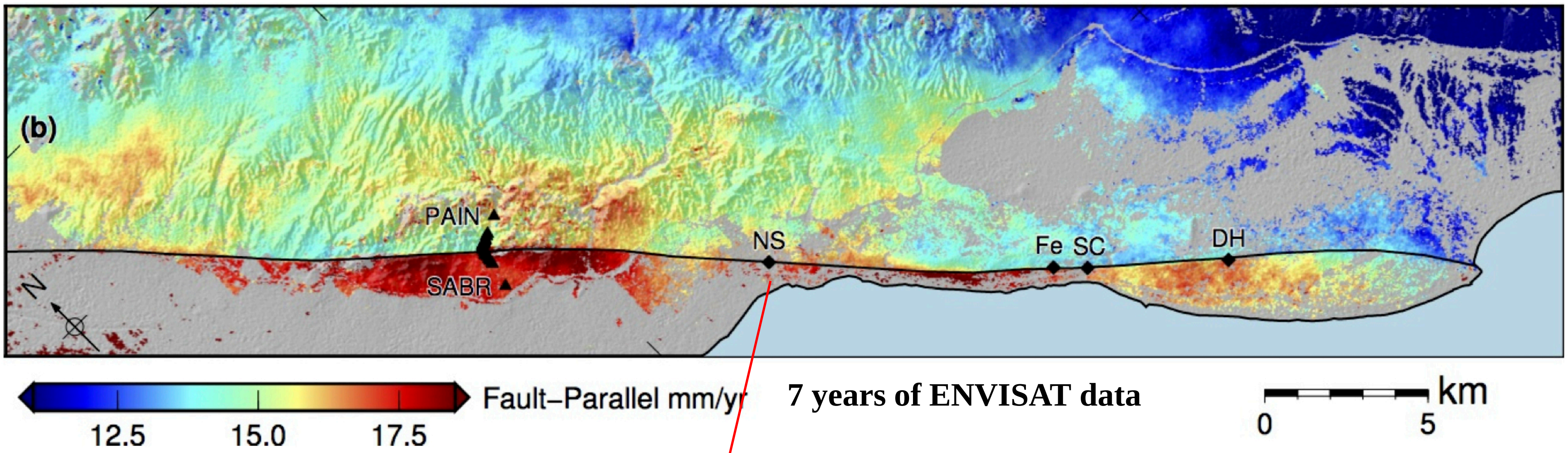

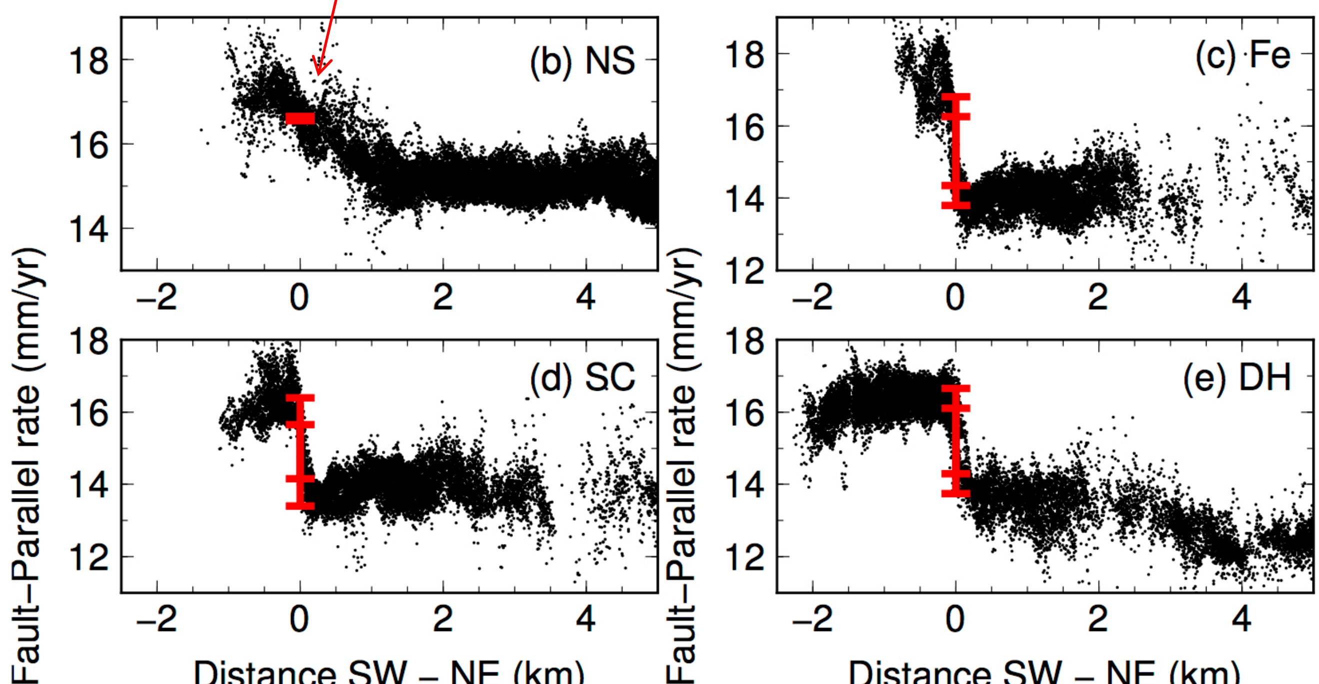

Lindsey et al.,
JGR 2014

Localized interseismic deformation: San Jacinto Fault zone

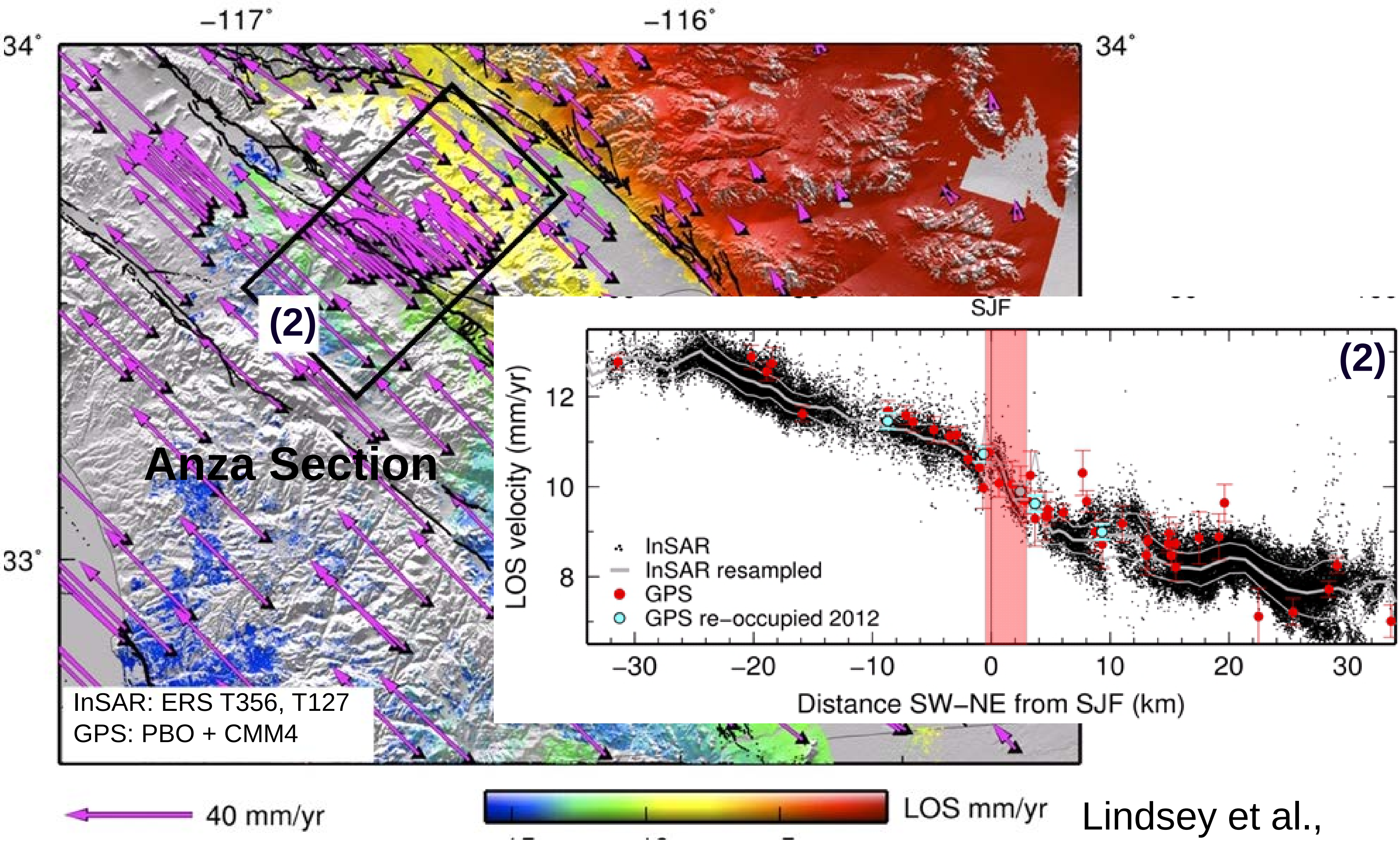

Lindsey et al., PAGEOPH 2014

An integral method to estimate the moment accumulation rate along the Creeping Section of the San Andreas Fault

High-pass filtered residual velocity estimate from ALOS and ERS. The velocity residuals across the creeping section are integrated to infer the moment deficit along the creeping fault.

ALOS

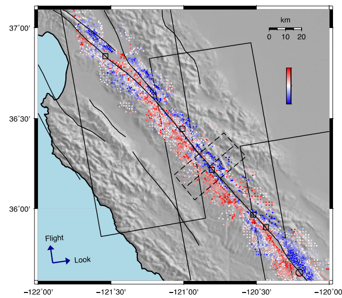

ERS

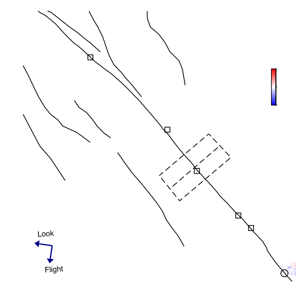

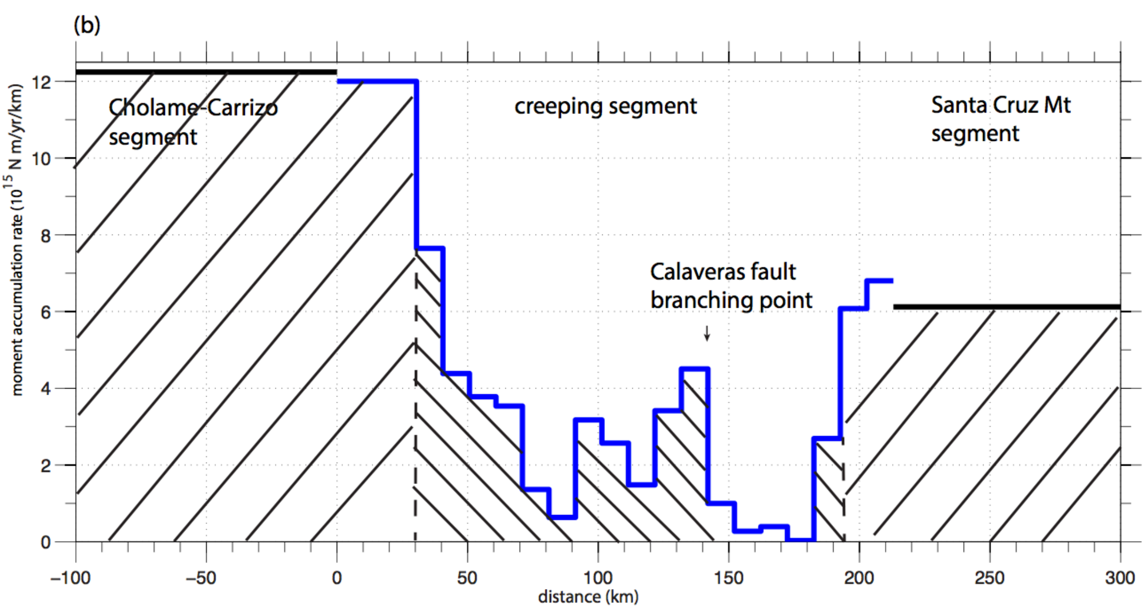

Along-strike variations of the moment accumulation rates for the Carrizo segment, Creeping Section and the Santa Cruz Mt. segment. The blue curves are determined by the InSAR velocity map.

[Tong et al., 2015, in review]

Potential for larger earthquakes in the San Francisco Bay Area due to the direct connection between the Hayward and Calaveras Faults

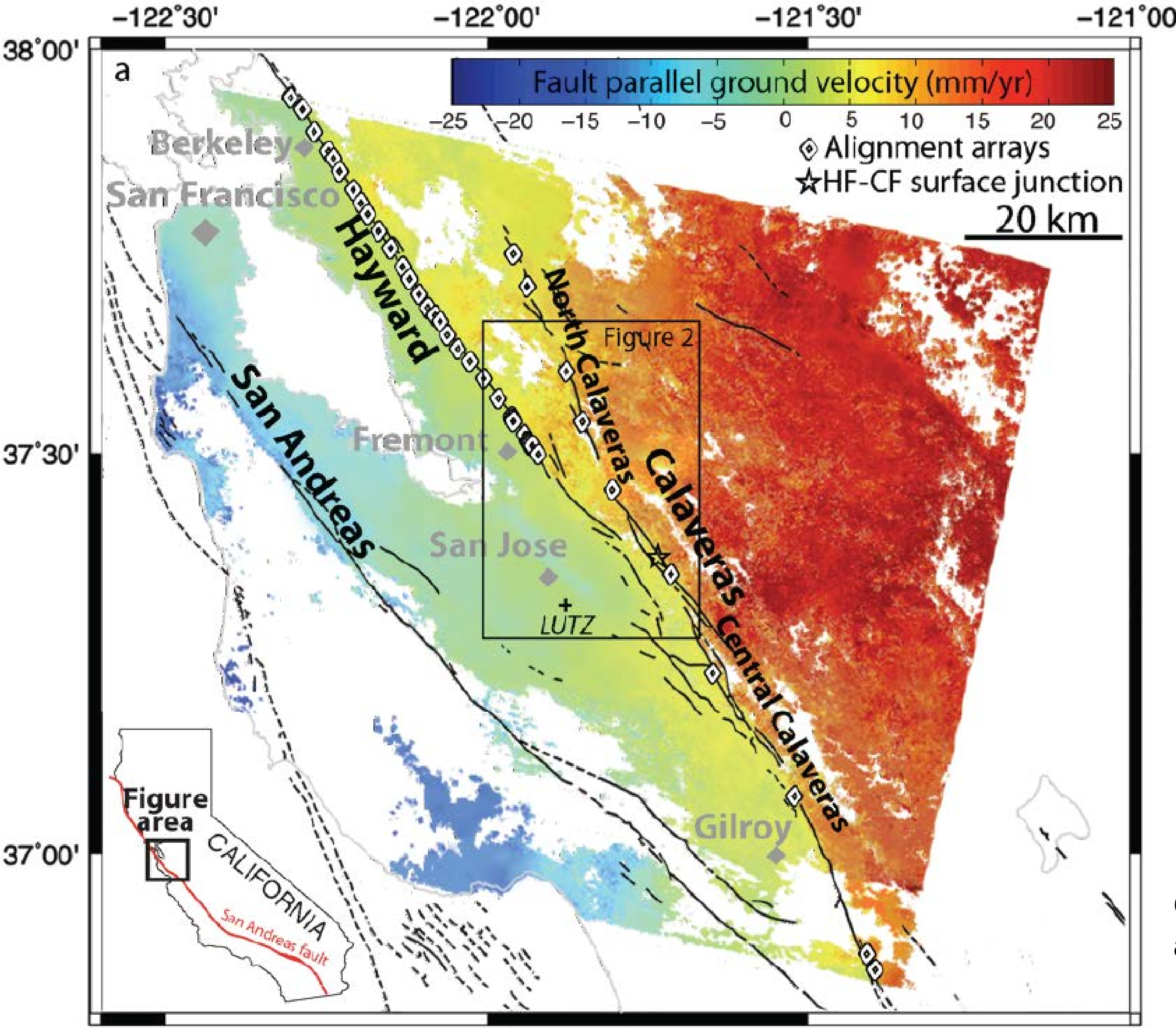

Mean HF-parallel ground velocity from 19 years of InSAR data in the San Francisco Bay Area. The sharp transitions in colors across the Hayward and Calaveras Faults document the interseismic surface creep.

Chaussard et, Burgmann, at al., GRL, in press

3. Earthquakes

Seismological and geodetic constraints on the 2011 Mw5.3 Trinidad, Colorado earthquake and induced deformation in the Raton Basin

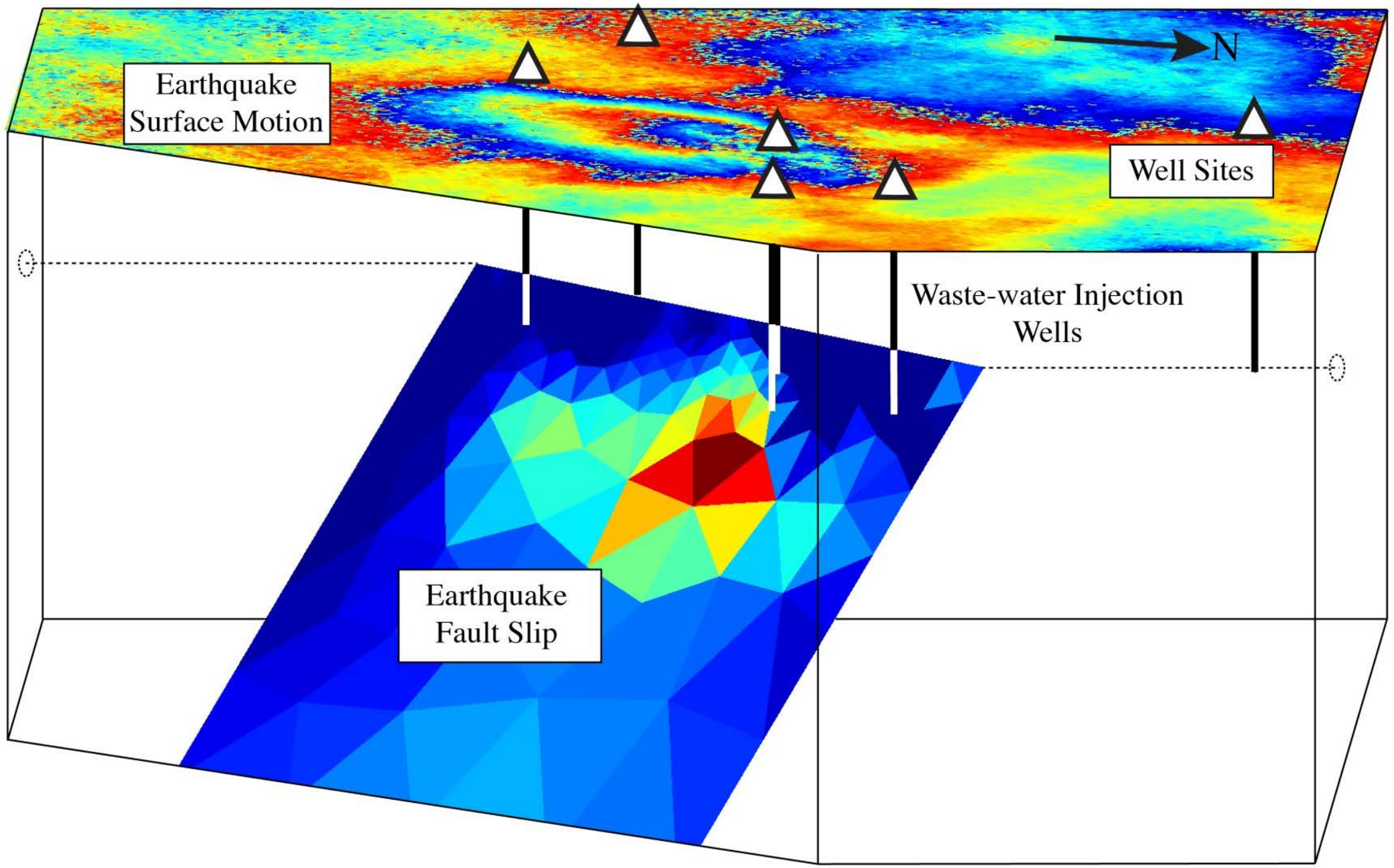

Barnhart et al., 2014

4. Inter-seismic and Post-seismic

Velocity map across the Chaman fault system, Pakistan & Afghanistan from 2004-2011 Envisat.

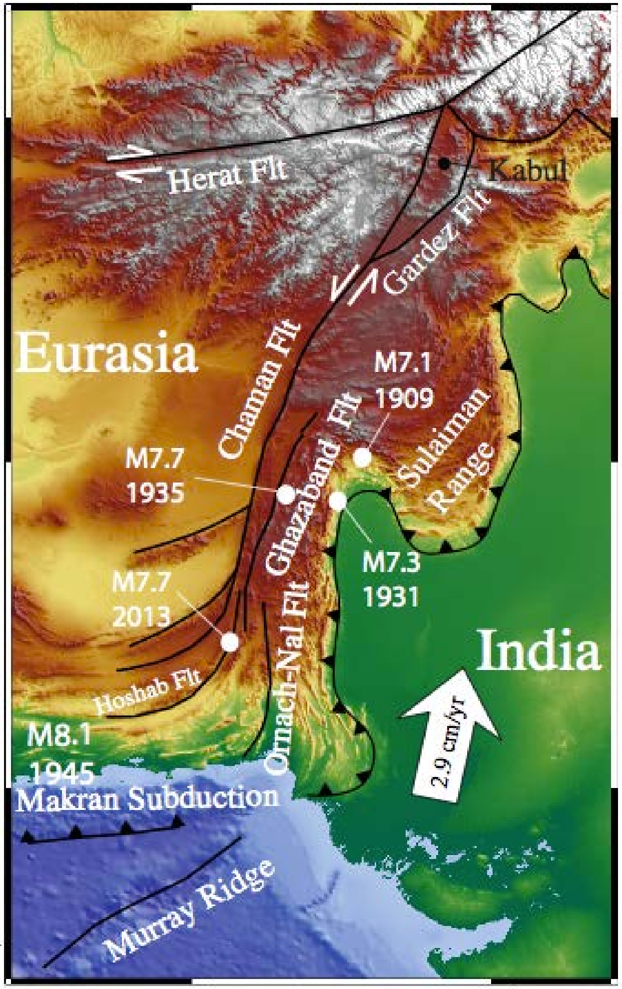

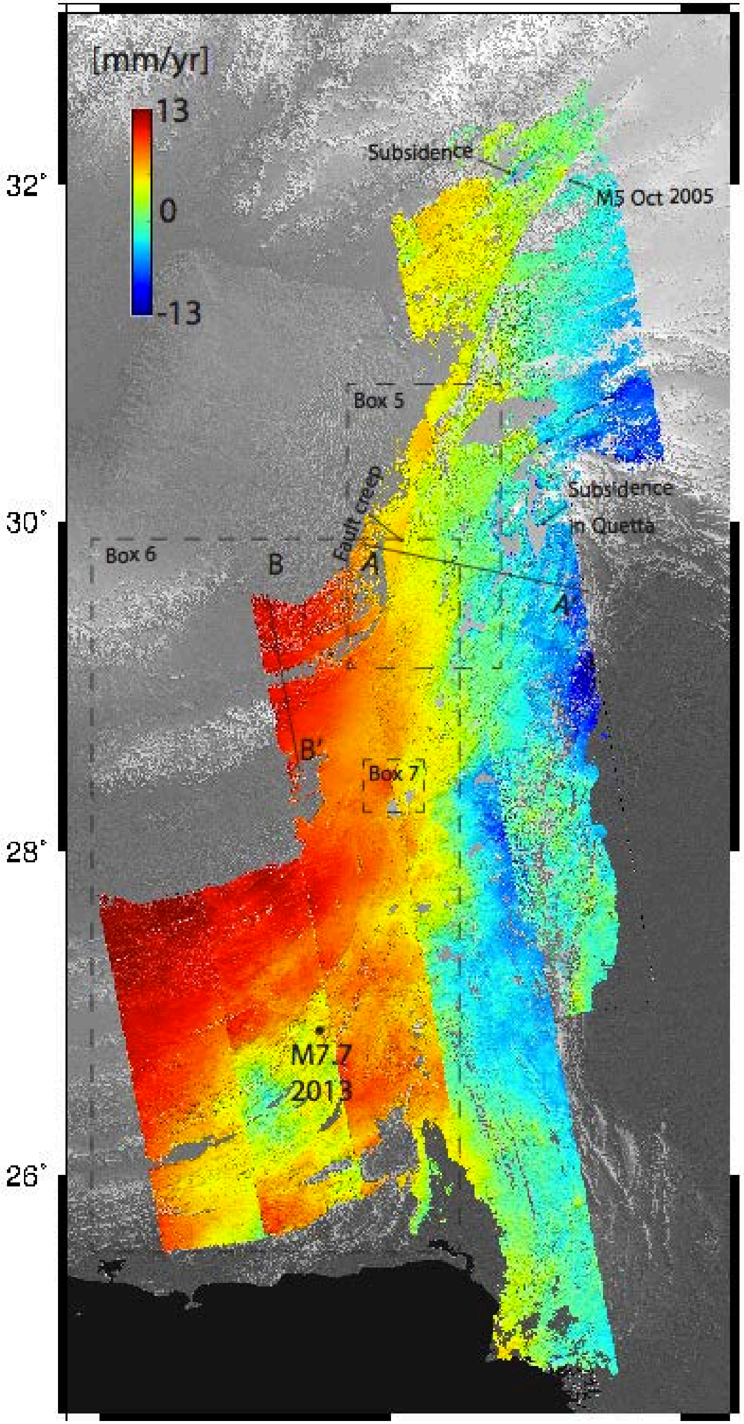

H. Fattahi and
F. Amelung, U of Miami

Post-seismic deformation due to the 2005 M7.6 Kashmir (Pakistan) earthquake

Wang and Fialko, JGR 2014

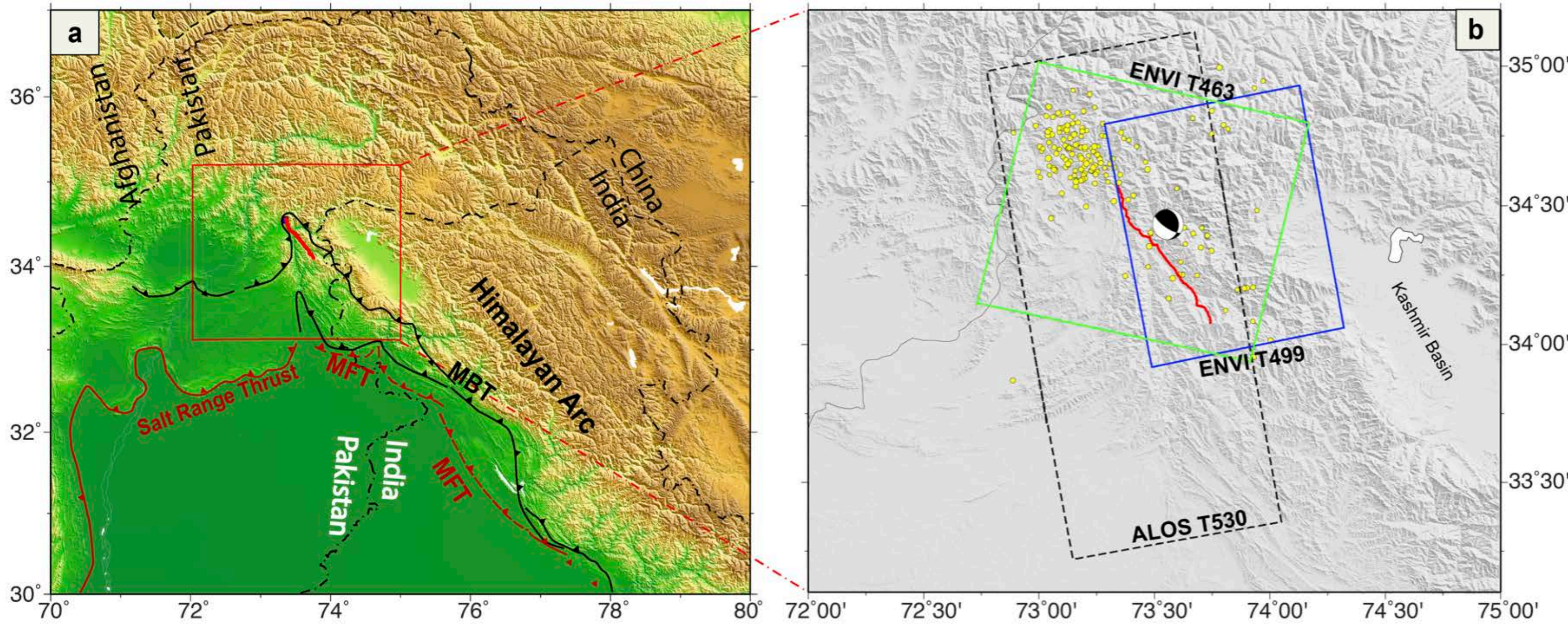

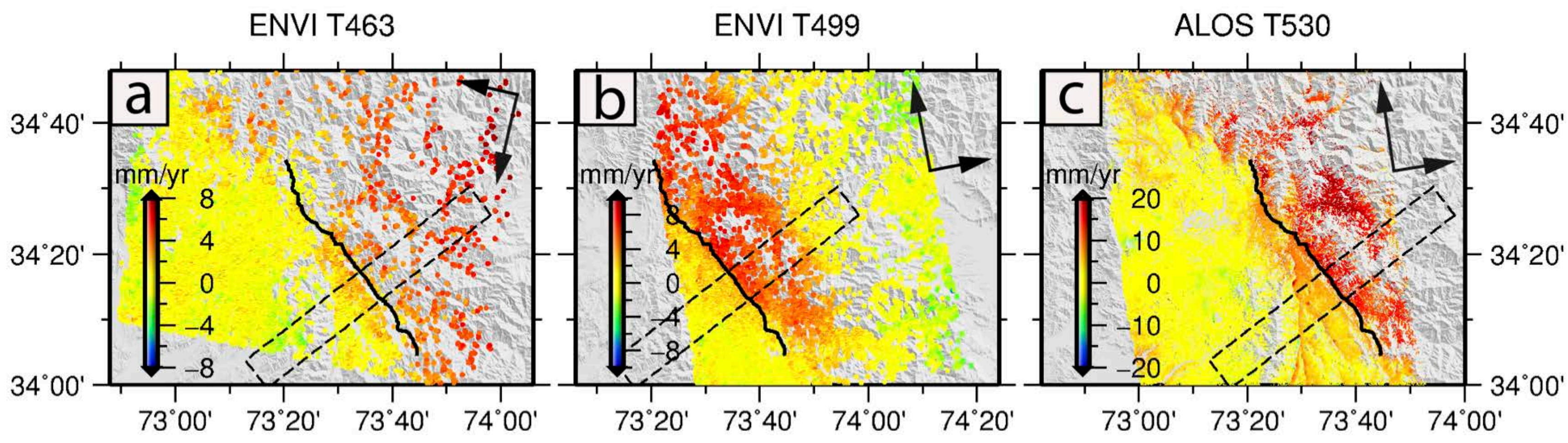

4. Subsidence

Using InSAR to document all anthropogenic deformation in the Western US

- We have cataloged over 200 locations of anthropogenic deformation, most of which are caused by groundwater removal.
- 42 of these signals are being documented for the first time in this study.
- The goal is to determine which GPS stations might be affected and the extent of anthropogenic change

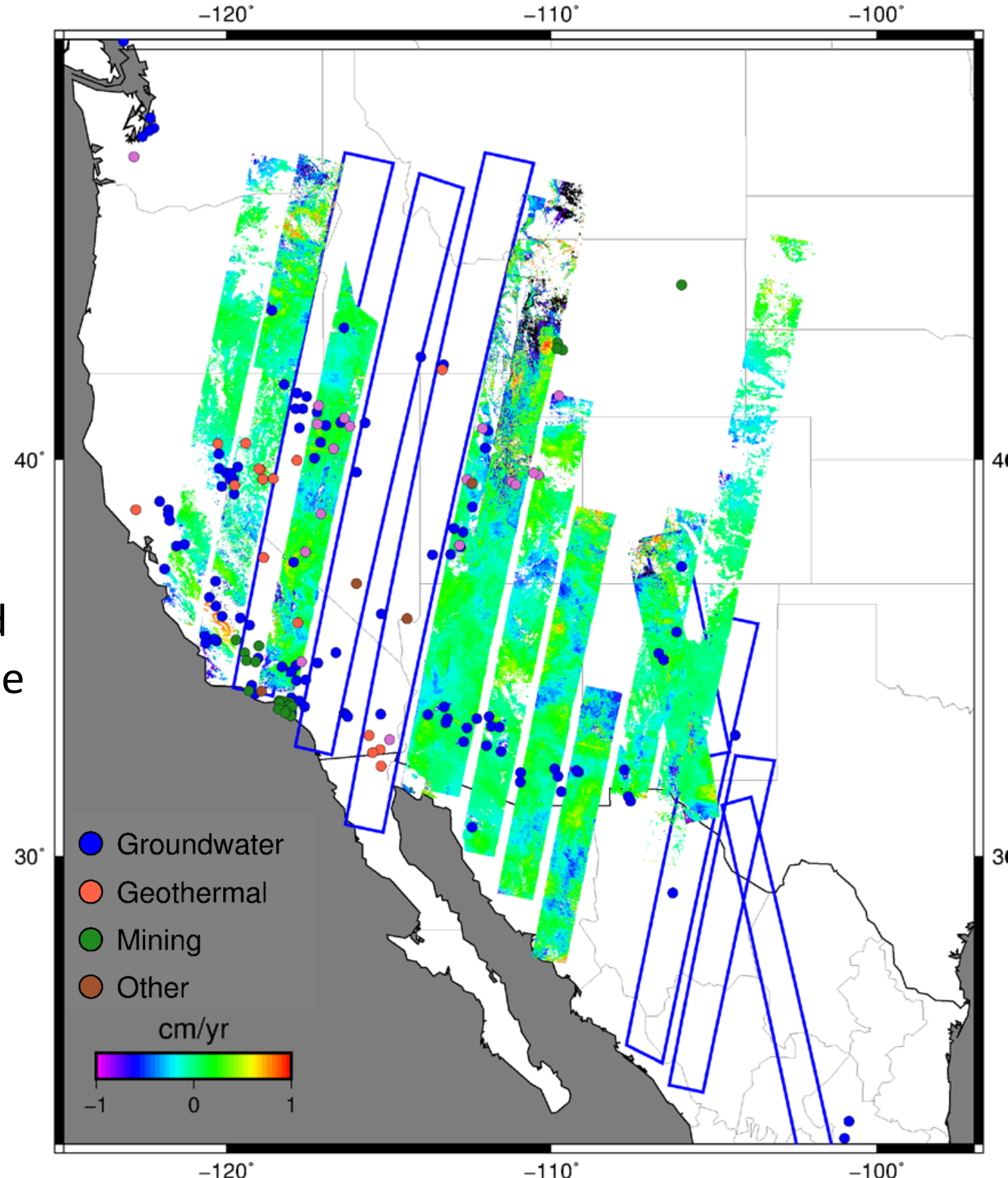

Credit: Matt Pritchard's group

Velocity map of the Basin & Range, from 1500 ERS frames, 1992-2000

F. Greene and F. Amelung, U of Miami

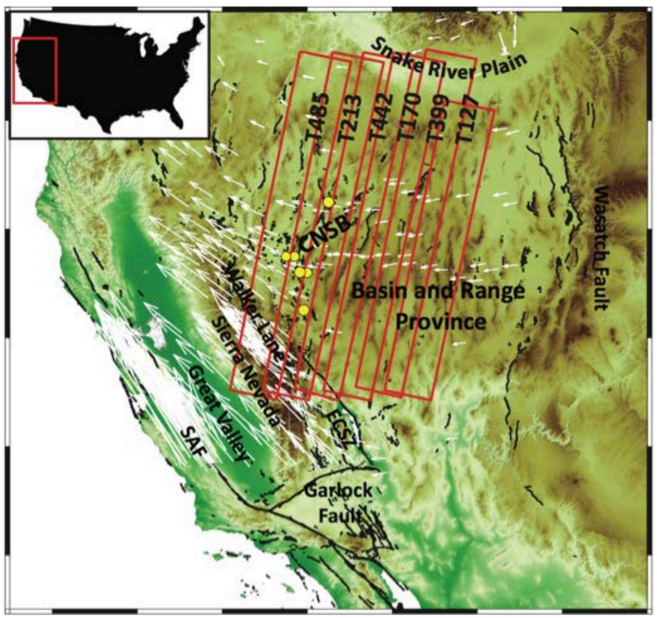

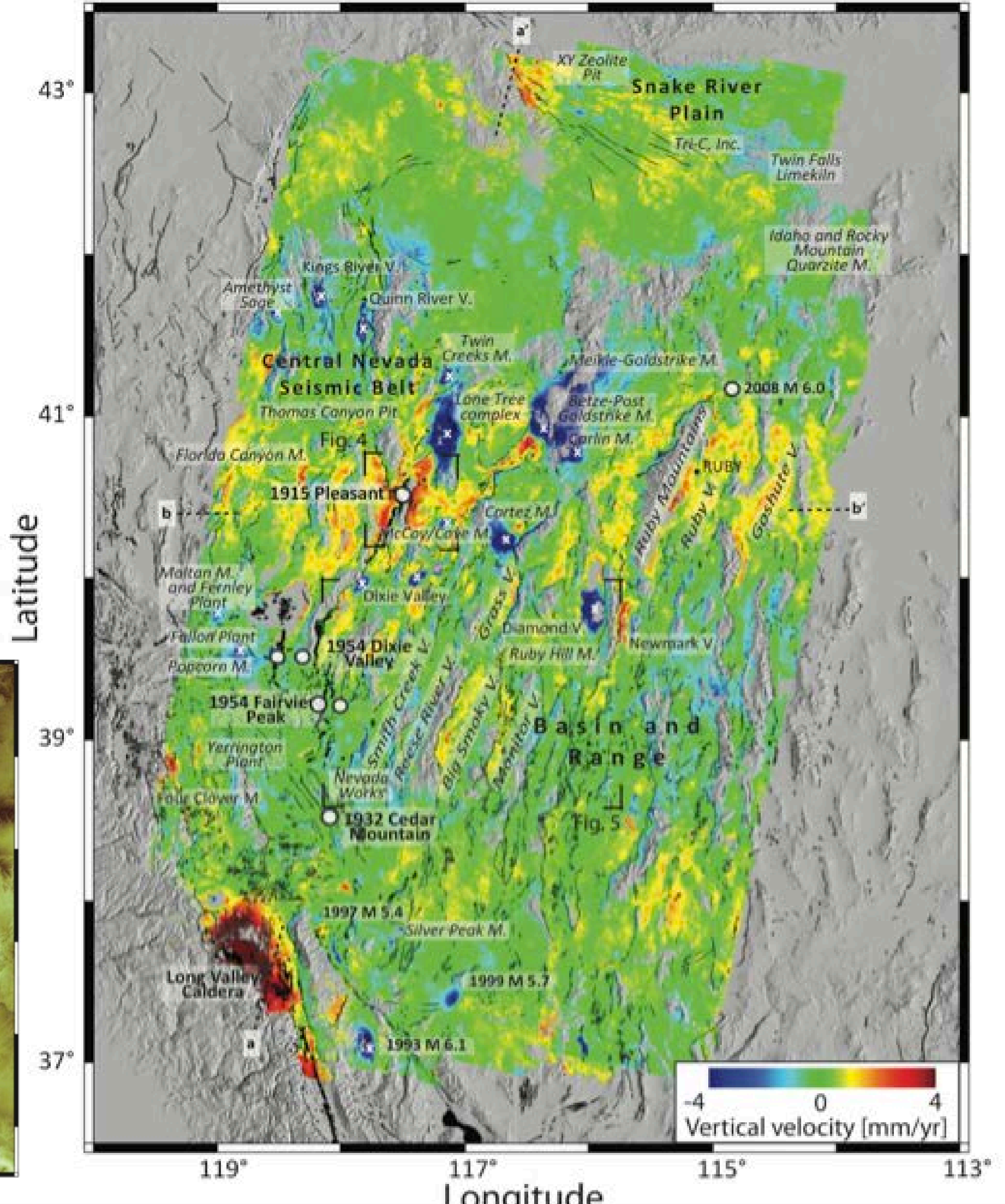

Ground Subsidence in Tucson, Arizona, Monitored by Time-Series Analysis Using Multi-Sensor InSAR Datasets from 1993 to 2011

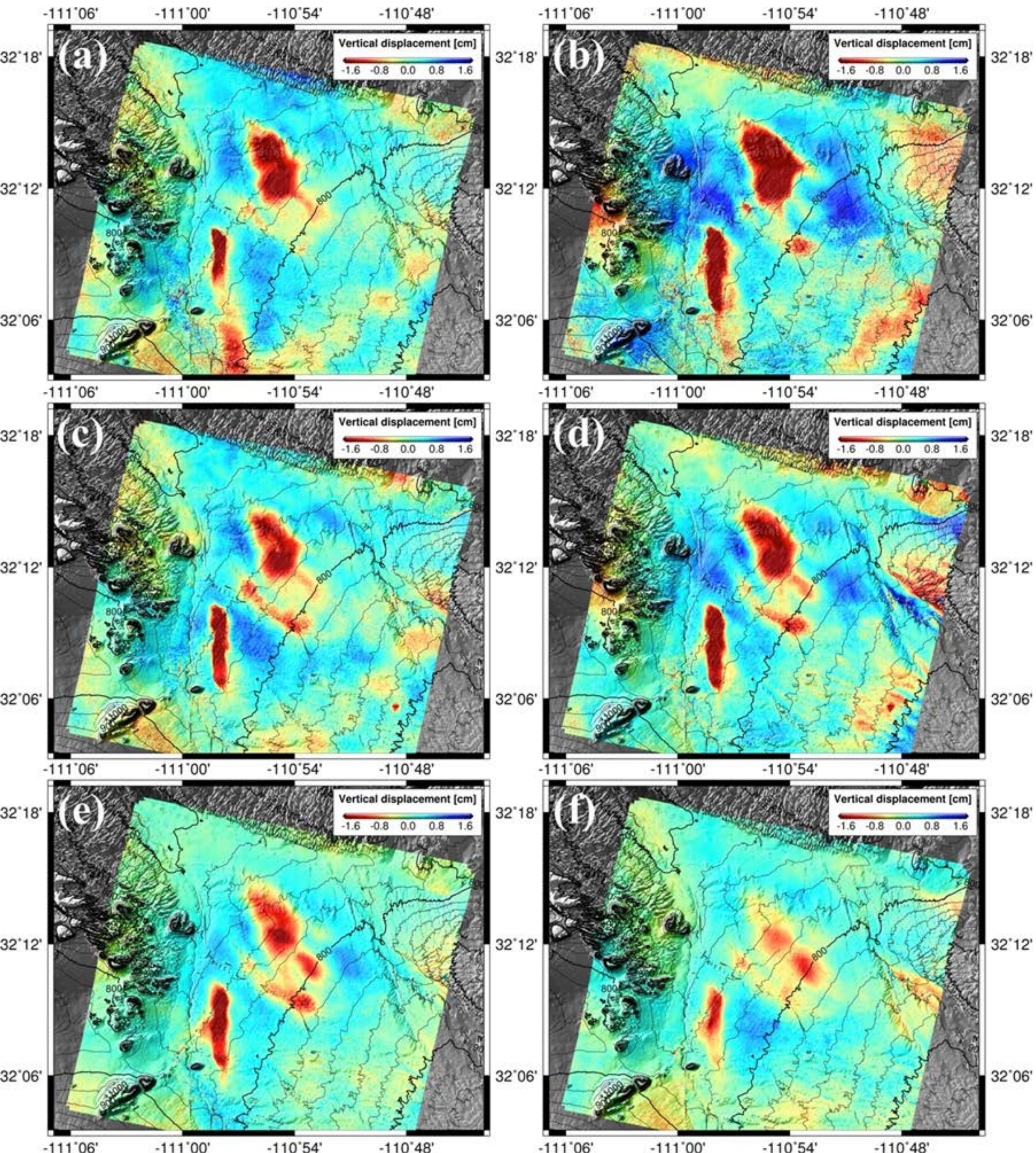

Three-year interval vertical deformation of (a) 1993.11.09 ~ 1996.11.22, (b) 1996.1122 ~ 1999. 11. 12, (c) 1999.11.12 ~ 2002.04.05, (d) 2002.04.05 ~ 2004.12.10, (e) 2004.12.10 ~ 2007.10.26, and (f) 2007.10.26 ~ 2010.09.10.

Kim, J.W., Z. Lu, Y.Y. Jia, J.W. Jones, C.K. Shum, Ground subsidence in Tucson, Arizona, monitored by time-series analysis using multi-sensor InSAR datasets from 1993 to 2011, *Journal of Photogrammetry and Remote Sensing*, *in press*, 2015.

SMU

GEODETIC SCIENCE
A DIVISION OF THE SCHOOL OF EARTH SCIENCES
THE OHIO STATE UNIVERSITY

Time series analysis of surface deformation at Brady Hot Springs geothermal field

Ali et al., 2014
U. Wisconsin-Madison

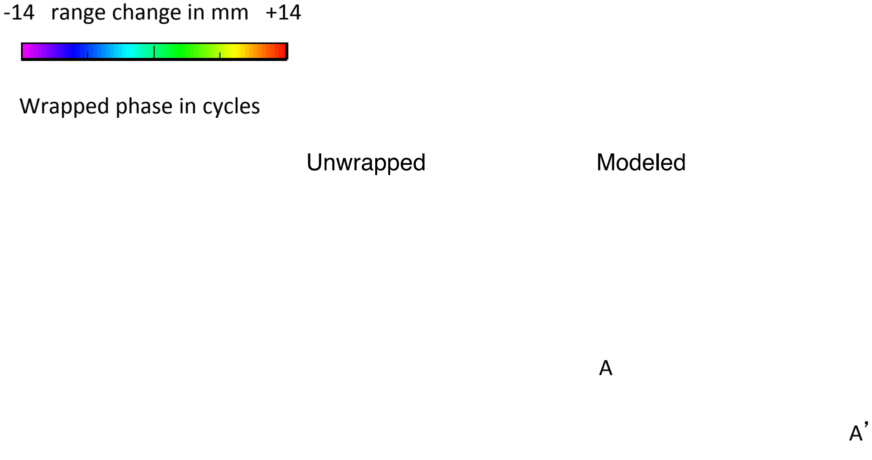

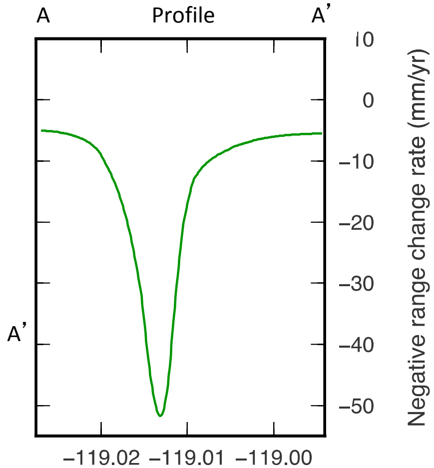

- **Subsidence is caused by contraction of rocks with relatively high fracture density, following decline in the temperature of water in the reservoir.**
- **Rate of observed deformation correlates well with production in shallow wells.**

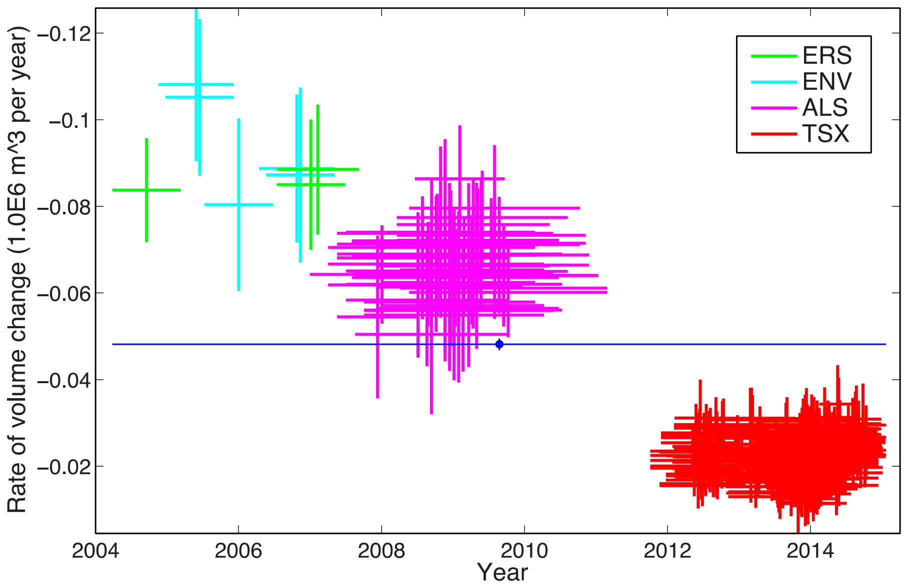

Rate of cumulative volume change, calculated from final estimate of parameters, along with uncertainties

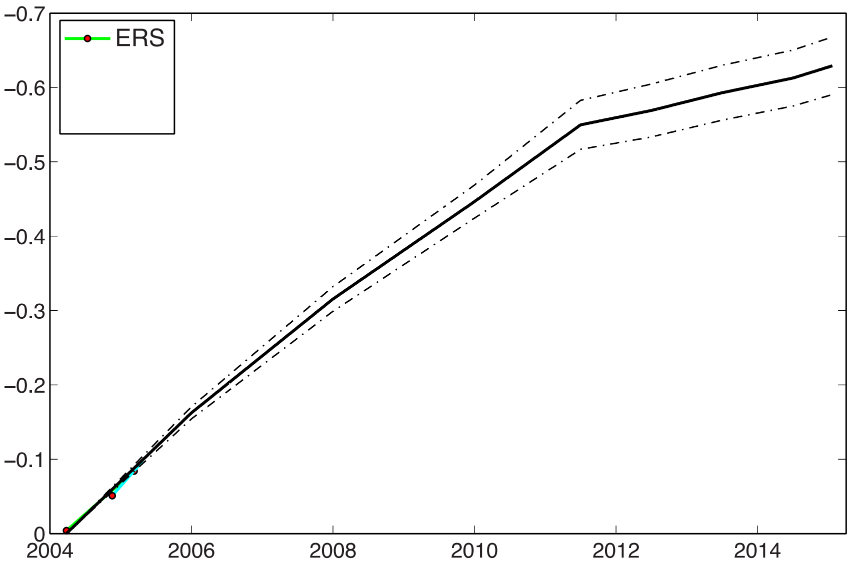

Volume change as a function of time as estimated from the individual pairs using temporal adjustment, assuming a piecewise linear model

InSAR used to image surface subsidence at the Cerro Prieto Geothermal Field

InSAR observations demonstrate that net fluid extraction at the CPGF causes surface subsidence at rates in excess of 10 cm/yr

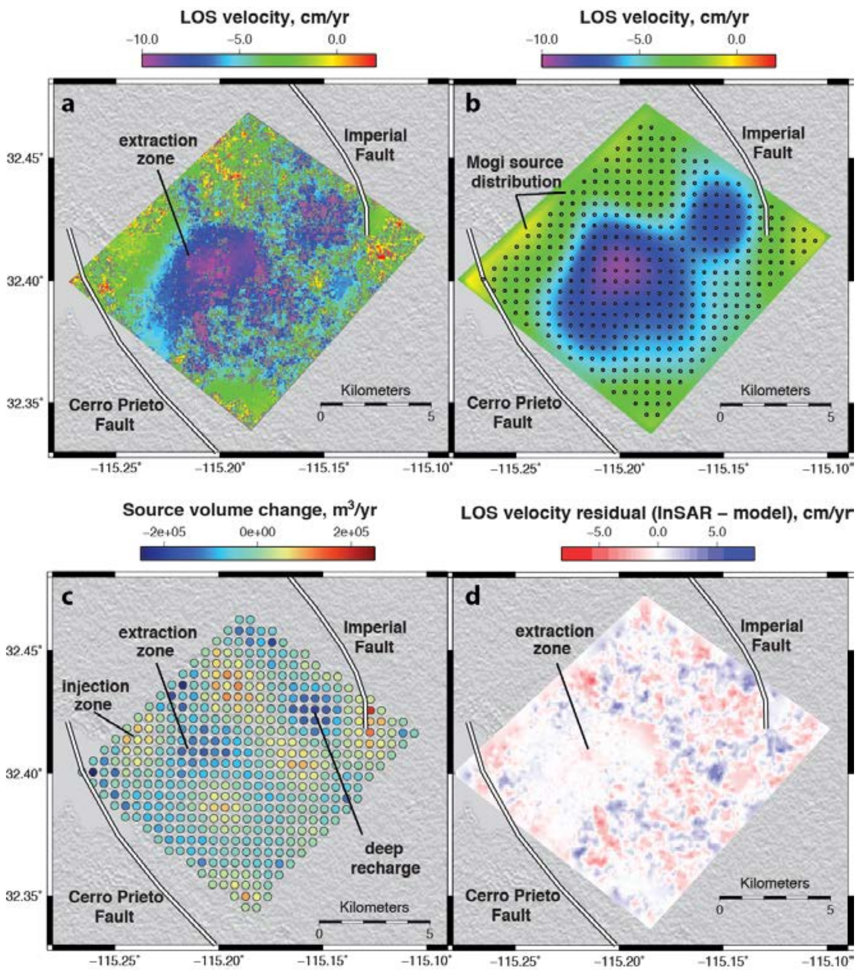

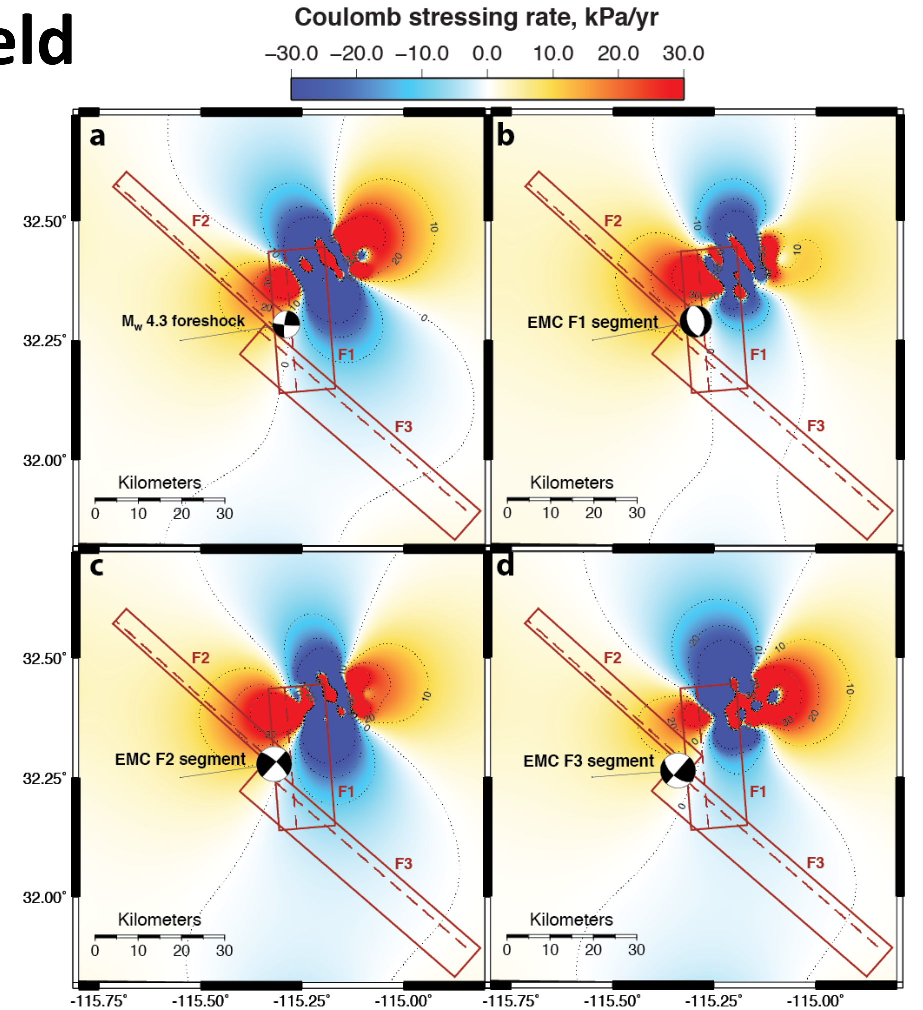

Geothermal production placed positive Coulomb stresses on the faults that ruptured in the 2010 M_w 7.2 El Mayor-Cucapah Earthquake sequence, priming them for failure.

Trugman et al., GRL, 2014

Predictability of hydraulic head changes and characterization of aquifer-system and fault properties from InSAR-derived ground deformation

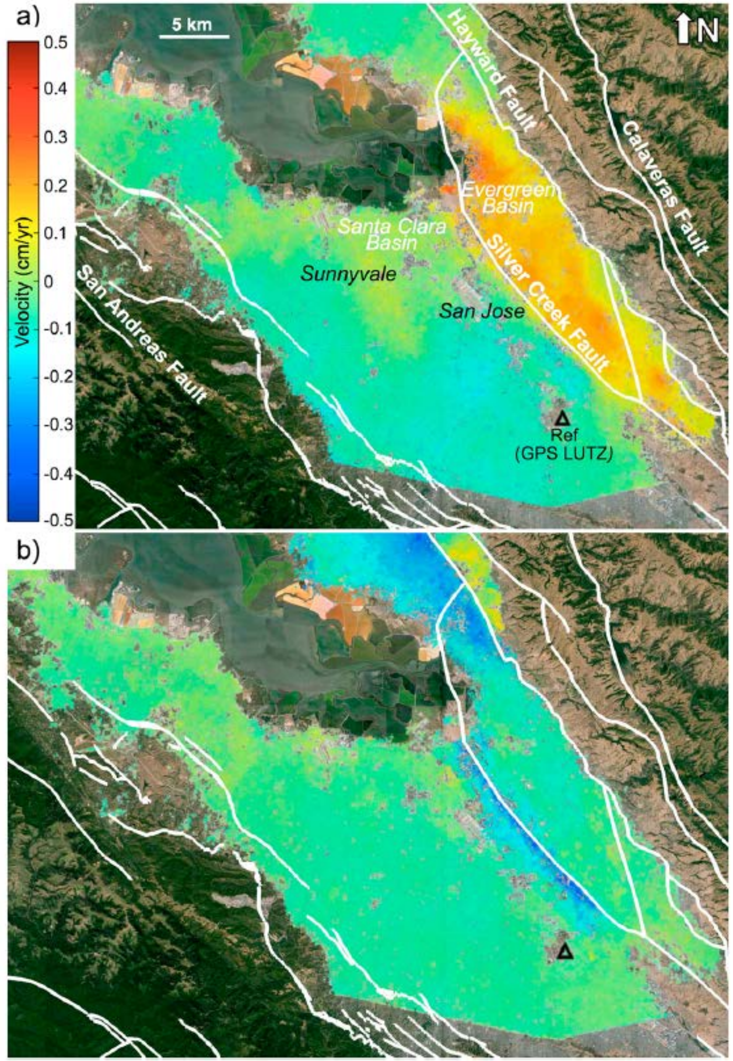

The 1992–2011 (a) averaged vertical and (b) east-west velocity maps in the Santa Clara Valley from ERS, Envisat, and ALOS InSAR SBAS time series. Credit: **Chaussard** et al., JGR 2014

5. Hydrological Studies

ASAR image analysis for detecting water cover changes over Chapala Lake influenced by seasonal variations

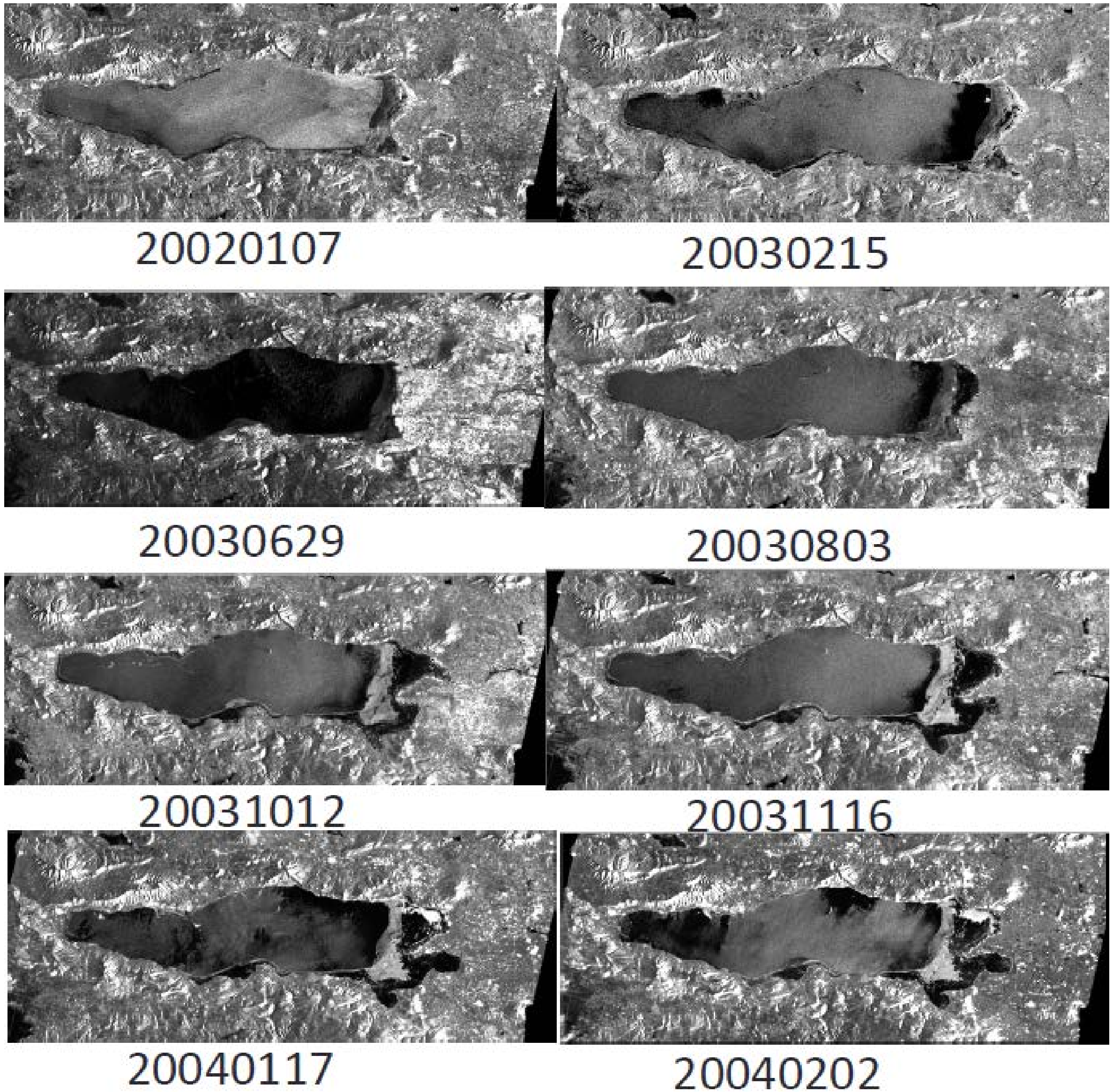

Credit: Damien O'Grady , Marc Leblanc, Adrian Bass, The use of radar satellite data from multiple incidence angles improves surface water mapping, Remote Sensing of Environment 140 (2014) 652–664.

Monitoring the Hydrology Changes in the Freshwater Marsh of the Everglades by Using L-band (ALOS-1_ Synthetic Aperture Radar Backscatter Coefficient

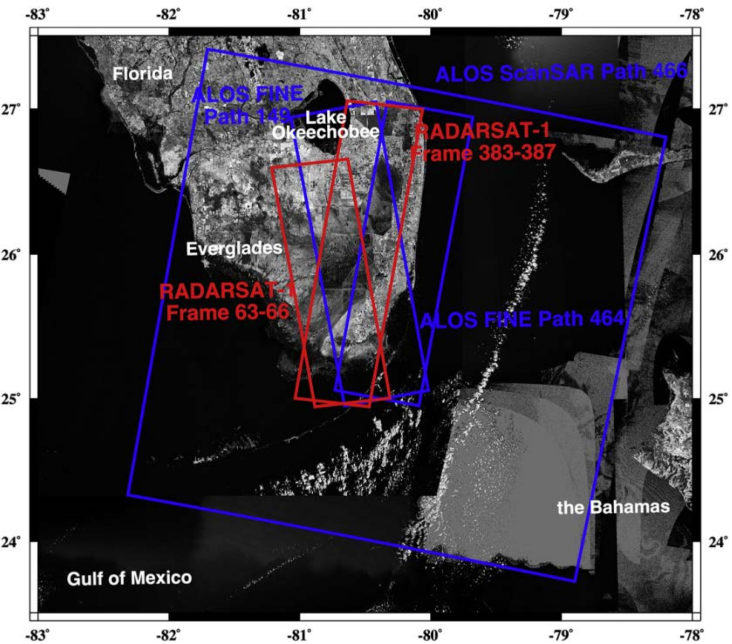

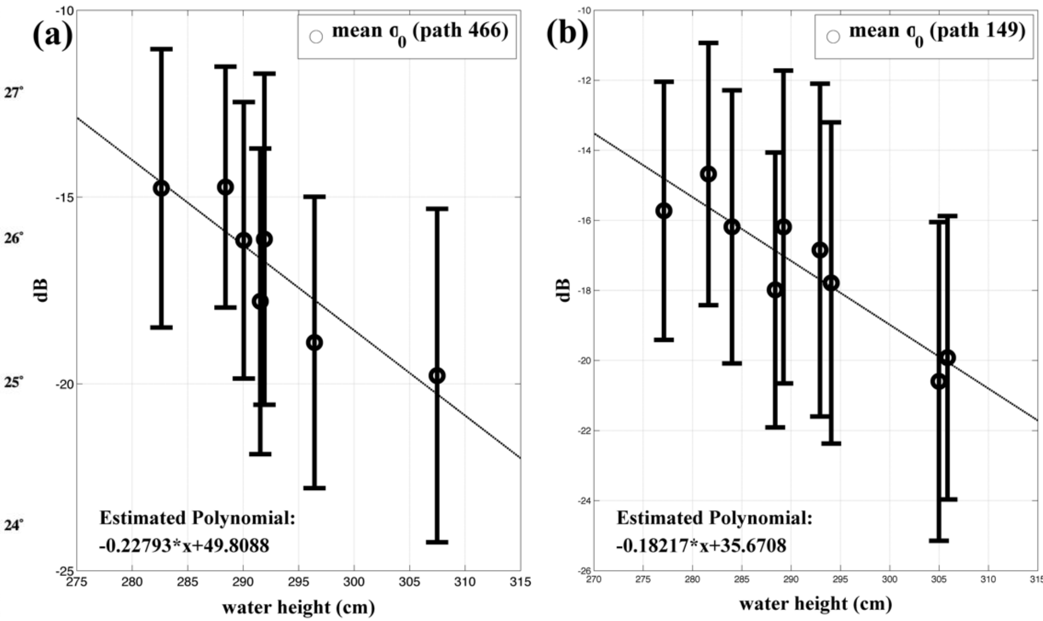

Mean backscattering coefficients from paths (a) 466 and (b) 149)and water height from each SAR date. Black circles represent averaged backscatter coefficient and length of error bars mean a standard deviation. Dotted lines are a linearly fit line from mean backscatter coefficient and water height.

Kim, J.W., Z. Lu, J.W. Jones, C. Shum, H.K. Lee, Y.Y. Jia, Monitoring everglades freshwater marsh water level using L-band synthetic aperture radar backscatter, *Remote Sensing of Environment*, 150, 66–81, doi:10.1016/j.rse.2014.03.031, 2014.

Estuary Tides Using ALOS-1/PALSAR Inferred Backscatter Water Level Measurements Over Sundarbans

(a)

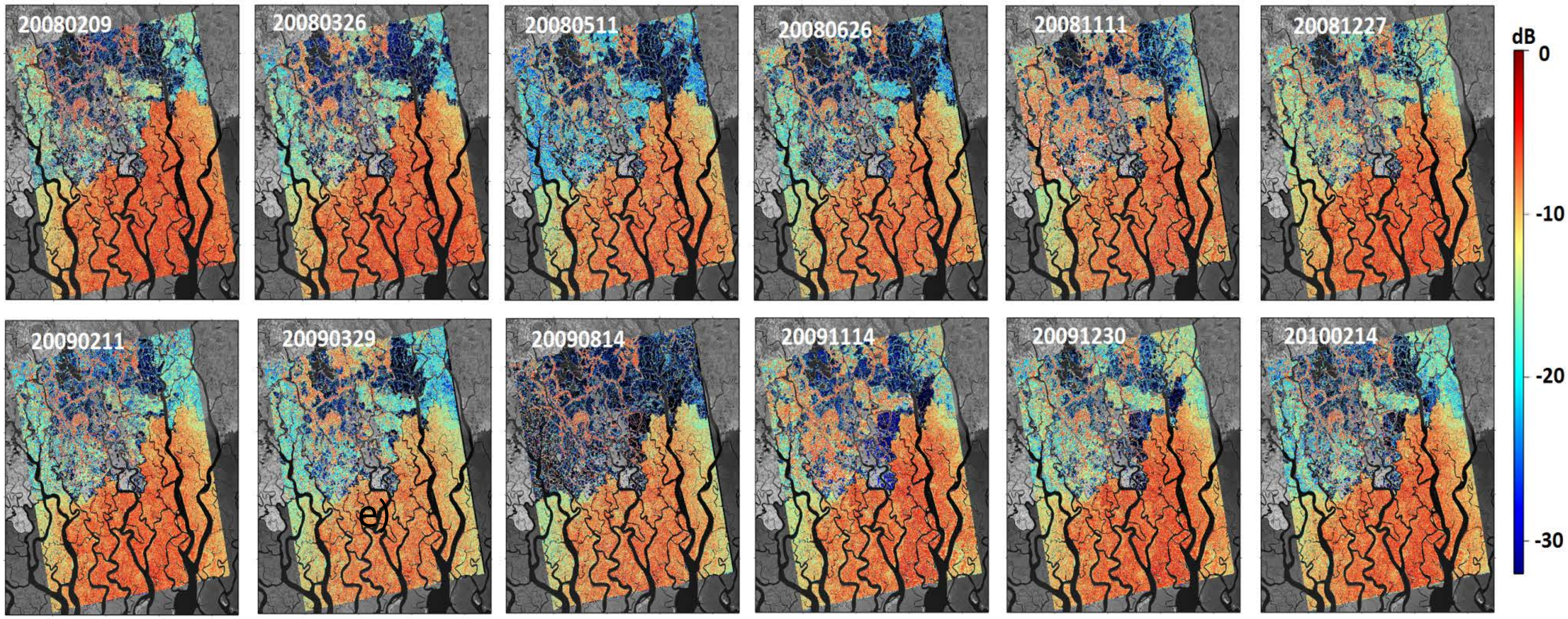

(b)

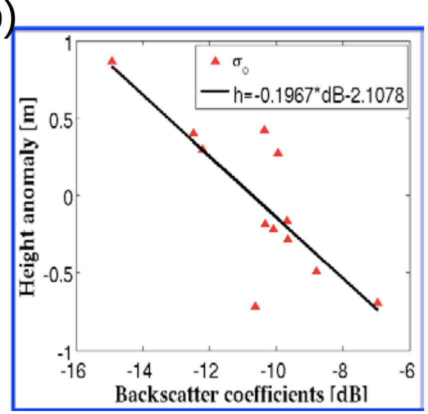

(c)

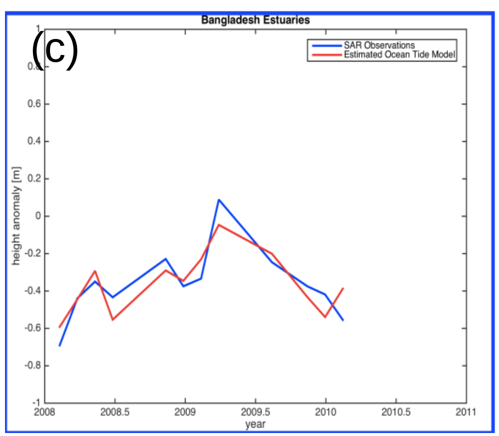

(a) ALOS backscatter coefficient maps from 20080209 to 20100214; (b) shows comparison between ALOS-1 PALSAR backscatter coefficients and height anomaly from Envisat altimetry observations. (c) The comparison between height anomaly computed from SAR backscatter coefficient and estimated ocean tide model. Despite ALOS-1's sun-synchronous and long (46-day) repeat-orbit, it is potentially feasible that some tidal constituents retrievable.

Yi, Y., C. Shum, J. Kim, Y. Jia, K. Tseng, K. Shang, S. Calmant, V. Ballu, L. Testut, Z.H. Khan, and X.C. Wang, Estuary tides using satellite altimetry and SAR/InSAR data, 2014 FALL AGU, San Francisco, December 15–19, 2014.

SMU GEODETIC SCIENCE A DIVISION OF THE SCHOOL OF EARTH SCIENCES THE OHIO STATE UNIVERSITY NASA

Thank you, ESA,
for the legendary ERS-1, ERS-2,
Envisat, Sentinel-1/A data sets
and more in the horizon !